Journal of the European Ceramic Society 22 (2002) 1811–1822

www.elsevier.com/locate/jeurceramsoc

# Microstructure and thermal expansion of $Al_2TiO_5$–$MgTi_2O_5$ solid solutions obtained by reaction sintering

L. Giordano[a,1], M. Viviani[a], C. Bottino[a], M.T. Buscaglia[a], V. Buscaglia[a,*], P. Nanni[b]

[a]*Institute of Physical Chemistry of Materials, National Research Council, via De Marini 6, I-16149 Genoa, Italy*
[b]*Institute of Process and Chemical Engineering, University of Genoa, Fiera del Mare, Pad. D., I-16146 Genoa, Italy*

Received 12 July 2001; received in revised form 5 November 2001; accepted 11 November 2001

**Abstract**

Solid solutions $Mg_{0.1}Al_{1.8}Ti_{1.1}O_5$ and $Mg_{0.5}AlTi_{1.5}O_5$ were obtained by reaction sintering of mixtures of the binary oxides at 1350–1600 °C using different precursor powders. For the composition $Mg_{0.1}Al_{1.8}Ti_{1.1}O_5$, ceramics sintered at 1400–1500 °C have high relative density (≥90%), reduced grain size (2–6 μm), low thermal expansion (−0.8 to $0.3\times10^{-6}$ $K^{-1}$ in the range 200–1000 °C) and reproducible expansion behaviour. At higher temperature, grain size rapidly increases owing to anisotropic and exaggerated grain growth (EGG) resulting in severe microcracking. Microstructure evolution is affected by the nature of the starting oxides, in particular for what concerns the onset temperature of EGG, the size and the fraction of abnormal grains. For the composition $Mg_{0.5}AlTi_{1.5}O_5$, EGG already takes place at 1350 °C and materials with grain size < 5 μm are difficult to obtain by conventional reaction sintering. Large grained samples (>10 μm) of both compositions show a reduced hysteresis and complex thermal expansion behaviour. In particular, heating to 1000 °C results in a significant increase in specimen size on return to room temperature. Repeated thermal cycling leads to an increase of the hysteresis. 

*Keywords:* $Al_2TiO_5$; Grain growth; Grain size; Microstructure-final; Thermal expansion

## 1. Introduction

Aluminium titanate ($Al_2TiO_5$) and magnesium dititanate ($MgTi_2O_5$) are ceramic oxides isostructural to the mineral pseudobrookite ($Fe_2TiO_5$, orthorhombic, S.G: Cmcm) characterized by an unusually high thermal expansion anisotropy. For $Al_2TiO_5$, the thermal expansion coefficients (TEC) along the principal crystallographic directions are, according to Bayer,[1] $\alpha_a = -2.9\times10^{-6}$ $K^{-1}$, $\alpha_b = 10.3\times10^{-6}$ $K^{-1}$, and $\alpha_c = 20.1\times10^{-6}$ $K^{-1}$ (Morosin and Lynch[2] have reported slightly different values: $\alpha_a = -1.4\times10^{-6}$ $K^{-1}$, $\alpha_b = 9.8\times10^{-6}$ $K^{-1}$, and $\alpha_c = 20.6\times10^{-6}$ $K^{-1}$). In the case of $MgTi_2O_5$, the TECs are: $\alpha_a = 2.3\times10^{-6}$ $K^{-1}$, $\alpha_b = 8.1\times10^{-6}$ $K^{-1}$ and $\alpha_c = 13.2\times10^{-6}$ $K^{-1}$.[1] During heating and cooling, thermal expansion anisotropy creates stresses between the grains of the polycrystalline ceramics and cooling from the sintering temperature can result in extensive internal microcracking. The connection between microcracking and thermal expansion anisotropy of aluminium titanate was firstly suggested by Buessem et al.[3] from the observation of the hysteresis loop of thermal expansion. Other than in linear expansion[4,5] materials with the pseudobrookite structure show hysteresis in thermal diffusivity,[6,7] strength, and elastic modulus.[5,8] Hysteresis in the elastic moduli and thermal expansion was also observed on other microcracked oxides, like $Nb_2O_5$,[9] $Eu_2O_3$,[10] $HfO_2$,[11] and $Ta_2WO_8$.[12] The anomalous behaviour arises because following crack closure and healing at high temperature, cooling over some temperature range is required before the internal stresses are high enough to reinitiate crack formation. An abrupt decrease of elastic modulus,[13] strength,[13] and linear expansion coefficient[14] with grain size has been reported in pseudobrookite polycrystalline ceramics. The different observations support the existence of a critical grain size. Below the critical size, the elastic energy available in the system is not sufficient to create microcracks during cooling from the sintering temperature and the polycrystalline body expands with

* Corresponding author. Tel.: +39-010-6475708; fax: +39-010-6475700.

*E-mail address:* buscaglia@icfam.ge.cnr.it (V. Buscaglia).

[1] Present address: Dip.to Scienza dei Materiali, Università di Milano La Bicocca, 20125 Milan, Italy.

0955-2219/02/$ - see front matter 
PII: S0955-2219(01)00503-9

a linear expansion coefficient $\overline{\alpha}=(\alpha_a+\alpha_b+\alpha_c)/3$. Above this value, elastic energy is spontaneously released by formation of cracks and the ceramic expands with an apparent TEC, $\alpha$, much lower than $\overline{\alpha}$. On subsequent heating most of the expansion of the individual grains is accommodated by the existing microcracks. On the basis of an energy criterion[13,15,16] or fracture mechanics,[17,18] different authors have shown that the critical grain size is inversely proportional to the product $(\Delta\alpha_{max}{}^2)(\Delta T^2)$. $\Delta\alpha_{max}$ is the maximum difference in thermal expansion among different directions. $\Delta T$ is the difference between the temperature at which the elastic stresses are no longer relieved by high-temperature plastic deformation and the temperature corresponding to the beginning of microcracking. The critical grain size at room temperature is evaluated to be in the range 1–2 μm for $Al_2TiO_5$ and 3–5 μm for $MgTi_2O_5$.[4,13,15]

Microcracked aluminium titanate ceramics exhibit low linear expansion coefficient ($\approx 10^{-6}$ $K^{-1}$), low thermal conductivity ($\approx$1.5 $Wm^{-1}$ $K^{-1}$), and excellent thermal shock resistance ($\approx$500 W $m^{-1}$). As a consequence, aluminium titanate is a candidate material for service conditions involving thermal shock resistance and good thermal insulation, like liners and manifolds in combustion engines, crucibles for molten aluminium, thermocouple protection tubes, nozzles, slides and tubes for metallurgy, etc. At high temperature (>1300 °C), the material can stand large macroscopic strains without significant microstructural changes.[19] However, a serious drawback of $Al_2TiO_5$ is its thermodynamic instability between 1280 and 900 °C.[20–23] To inhibit decomposition in the parent oxides, different stabilizers (MgO, $Fe_2O_3$, $ZrO_2$, $SiO_2$) have been proposed.[20] The addition of MgO leads to the formation of a $Al_2TiO_5$–$MgTi_2O_5$ solid solution of composition $Al_{2(1-x)}Mg_xTi_{(1+x)}O_5$, where $x$ is the molar fraction of $MgTi_2O_5$.[21] A substantial amount of MgO (10–25 mol%) is required to significantly increase the lifetime of ceramic components, even though long-time stabilization of aluminium titanate in the range 1000–1100 °C is still an open problem.[22,23] Sintered materials are usually prepared from aluminum titanate powders or directly by reaction sintering of mixtures of $Al_2O_3$, $TiO_2$, and stabilizing oxides. Microstructure is strongly affected by the amount and the nature of the stabilizing additive and also by the impurities contained in the raw materials.[24–26] In our opinion this is the main reason why a large variability of the thermal hysteresis curve is observed in the available literature even when the average grain size is greater than the critical one for microcracking.

In the present paper, we have examined a number of ceramics over a wide range of grain size (2–100 μm) for two different $Al_{2(1-x)}Mg_xTi_{(1+x)}O_5$ solid solutions: $x=0.1$ and $x=0.5$. This study is aimed to correlate the evolution of microstructure and thermal expansion behaviour with composition and sintering temperature.

## 2. Experimental

Solid solutions with composition $Al_{1.8}Mg_{0.1}Ti_{1.1}O_5$ ($x=0.1$) and $AlMg_{0.5}Ti_{1.5}O_5$ ($x=0.5$) were prepared by a solid-state route starting from $Al_2O_3$, $TiO_2$, and MgO. Some characteristics of the parent oxide powders are reported in Table 1. The powders were mixed inside polyethylene jars using deionized water and alumina media. A fully-organic deflocculant (Suspensil SM, Lamberti CMC, Italy) and a polysaccharide binder (Resigel, Lamberti CMC, Italy) were added during the mixing process. Before mixing, MgO powders were calcined at 500 °C for 2 h. After drying and sieving (40 mesh), compact cylindrical bodies (Ø = 1 cm, $L=10$ cm) were formed by cold isostatic pressing at 150 MPa. Sintered materials were finally obtained by firing at temperatures between 1350

Table 1
Powder properties

| | Oxide | Type | Purity | Predominant phase | BET surface ($m^2g^{-1}$) | $d$ (μm) |
|---|---|---|---|---|---|---|
| A1 | $Al_2O_3$ | Baikowski CR6 Lot 1134N | 99.99 | α | 6.6 | 0.23[a] |
| A2 | $Al_2O_3$ | Baikowski CR15 Lot 1059M | 99.99 | α | 14.6 | 0.10[a] |
| T1 | $TiO_2$ | Aldrich, 22422-7 Lot 07631TR | 99.9 | Rutile | – | ≈1[b] |
| T2 | $TiO_2$ | Cookson-Mattey AT1 | 99.9 | Anatase | – | ≈0.2[b] |
| M1 | MgO | Aldrich, 24388-8 Lot 19124 MQ | 98 | Periclase | 5.5 | 0.30[a] |
| M2 | MgO | Aldrich, 34279-3 Lot 11102AX | 99 | Periclase | 102 | 0.016[a] |

[a] From BET surface area.
[b] From SEM observation.

and 1600 °C, for 2 h, in air. The heating rate was 3 °C $min^{-1}$. During heating, an isothermal treatment at 300 °C for 5 h allowed for the burnout of the organic additives. Eight series of ceramic samples were prepared by different combinations of the starting oxides. The designation of the ceramics is shown in Table 2. Two additional samples of the series M1-3 ($x = 0.1$) were sintered at 1600 °C for 24 and 100 h, respectively, to promote grain growth. For comparison sake, some ceramics containing a small amount of MgO ($x = 0.01$) were also prepared. The apparent density of sintered specimens was measured by immersion in water. A thin gloss layer was applied on the samples to avoid water absorption. The reference densities are 3.70 g $cm^{-3}$ for $Al_2TiO_5$ and 3.65 g $cm^{-3}$ for $MgTi_2O_5$. Microstructure was observed by scanning electron microscopy (SEM, model 515, Philips, The Netherlands) after usual ceramographic preparation. Quantitative microstructure characterisation was carried out on a selected number of samples, in order to study the effect of raw materials for a given sintering temperature (1500 °C) and the effect of sintering temperature (from 1400 to 1600 °C) at a fixed composition (M1-3 and M5-3 series). For each sample, grain size distribution and shape factor distribution were obtained with the aid of an image analysis software (AnalySIS, Soft Imaging System, Germany). The grain size frequency distribution (GSFD) was estimated on the basis of 300–500 grains. Chemical etching with a HF aqueous solution (15%) was employed to improve detection of grain boundaries. The coefficient of thermal expansion between 200 and 1000 °C was measured using a dilatometer (SetSys 24, Setaram, France) at a constant heating and cooling rate of 3 °C/min.

## 3. Results

### 3.1. Microstructure

The apparent relative density of the different ceramics is shown in Fig. 1 as a function of the sintering temperature. The density generally increases as sintering temperature increases. Only samples M5-2 are quite insensitive to temperature. The density is significantly affected by the nature of the raw materials. When the combination of starting oxides A1 + T1 is used, the final density is strongly dependent on the kind of magnesium oxide (compare, for example, series M5-1 and M5-2). On the contrary, when the combination A2 + T2 is adopted, the influence of magnesium oxide is less pronounced. Samples containing 1 mol% MgO (not shown in Fig. 1) have a rather constant density (87–90%) irrespective of raw materials and sintering temperature. SEM observation has revealed that the formation of the titanate solid solution is not yet complete at 1350 °C after 2 h since many small isolated $Al_2O_3$ and $TiO_2$ particles are present. Some parent oxide particles are also observed on samples M1-2, M5-2, and M5-4 sintered at 1400 °C. The results of microstructure characterization are reported in Table 3. The data columns represent: the relative density, the average grain size ($S_A$), the size corresponding to the maximum frequency of the distribution ($S_{MF}$, the mode of the distribution), the average shape factor of the grains ($F_A$), the percentage (number base) of grains with size $> 3S_{MF}$ and the percentage (number base) of grains with $F > 2.5$. The shape factor is defined by the ratio between the two principal axes of the grain section. The average grain size is that corresponding to the mean of the distribution. Since most samples show non-equiaxed grains, the size of each grain was defined as the sum of the length of the two principal axes of the grain section divided by 2. The variation of the average grain size is from 2.3 to 19.5 μm for the solid solution $x = 0.1$ and from 4.4 to 42 μm for the solid solution $x = 0.5$ for a sintering time of 2 h. Some typical microstructures are shown in Fig. 2 (M1-3, 1400 °C), Fig. 3 (M1-3, 1500 °C), Fig. 4 (M1-4, 1500 °C), Fig. 5 (M5-1, 1450 °C) and Fig. 6 (M5-3, 1500 °C). Microstructure evolution with temperature is dominated by anisotropic grain growth, i.e. the growth of elongated grains. In the case of M1-3 ceramics, $F_A$ increases from 1.3 after 2 h sintering at 1400 °C to 2 after 100 h sintering at 1600 °C. Samples with an average shape factor > 1.6 have a significant percentage of

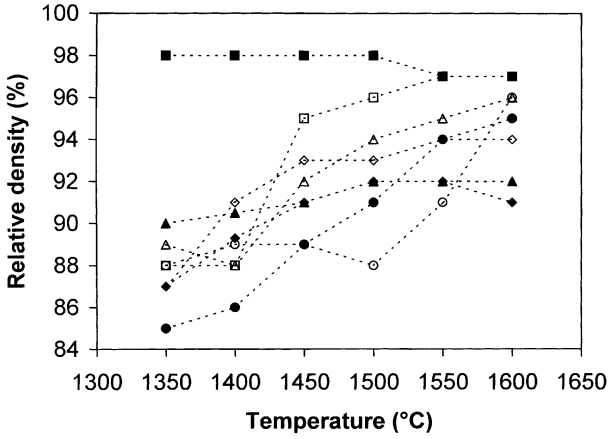


Fig. 1. Relative density of solid solutions $Mg_{0.1}Al_{1.8}Ti_{1.1}O_5$ and $Mg_{0.5}AlTi_{1.5}O_5$ sintered at different temperatures. (○)M1-1, (□)M1-2, (△)M1-3, (◇)M1-4, (●)M5-1, (■)M5-2, (▲)M5-3, (◆)M5-4. For identification of samples, see Table 2.

Table 2
Constitution of ceramic samples

| $Al_{1.8}Mg_{0.1}Ti_{1.1}O_5$ | | $AlMg_{0.5}Ti_{1.5}O_5$ | |
|---|---|---|---|
| Name | Formulation | Name | Formulation |
| M1-1 | A1 + T1 + M1 | M5-1 | A1 + T1 + M1 |
| M1-2 | A1 + T1 + M2 | M5-2 | A1 + T1 + M2 |
| M1-3 | A2 + T2 + M1 | M5-3 | A2 + T2 + M1 |
| M1-4 | A2 + T2 + M2 | M5-4 | A2 + T2 + M2 |

Table 3
Microstructure of sintered samples. $S_A$: average grain size; $S_{MF}$ mode of grain size distribution; $F_A$: average shape factor. Standard deviations are indicated in brackets

| Sample | Relative density (%) | $S_A$ (μm) | $S_{MF}$ (μm) | $F_A$ | Percentage of grains with $S>3S_{MF}$ | Percentage of grains with $F>2.5$ |
|---|---|---|---|---|---|---|
| $Al_{1.8}Mg_{0.1}Ti_{1.1}O_5$ | | | | | | |
| M1-1 (1500 °C/2 h) | 88 | 3.3 (0.8) | 3 | 1.33 (0.28) | 0 | 0 |
| M1-2 (1500 °C/2 h) | 96 | 14 (14) | 6 | 1.6 (0.6) | 20 | 8 |
| M1-3 (1400 °C/2 h) | 88 | 2.3 (0.5) | 2 | 1.3 (0.2) | 0 | 0 |
| M1-3 (1450 °C/2 h) | 92 | 3.8 (1.5) | 3 | 1.65 (0.57) | 0 | 9 |
| M1-3 (1500 °C/2 h) | 94 | 6.3 (3.1) | 5.5 | 1.72 (0.65) | <1 | 12 |
| M1-3 (1550 °C/2 h) | 95 | 15.0 (14) | 7 | 1.69 (0.67) | 24 | 9 |
| M1-3 (1600 °C/2 h) | 96 | 19.5 (17) | 14 | 1.83 (0.66) | 5 | 16 |
| M1-3 (1600 °C/24 h) | – | 79.2 (68) | 52 | 1.93 (0.71) | 6 | 17 |
| M1-3 (1600 °C/100 h) | – | 111 (86) | 70 | 2.02 (1.04) | 5 | 19 |
| M1-4 (1500 °C/2 h) | 93 | 9.3 (6.5) | 5 | 1.76 (0.76) | 13 | 12 |
| $AlMg_{0.5}Ti_{1.5}O_5$ | | | | | | |
| M5-1 (1450 °C/2 h) | 89 | 4.4 (1.4) | 4.5 | 1.4 (0.29) | 0 | 0 |
| M5-1 (1500 °C/2 h) | 91 | 8.8 (3.4) | 8 | 1.42 (0.38) | 0 | 4 |
| M5-2 (1500 °C/2 h) | 98 | 31 (24) | 22 | 1.70 (0.71) | 7 | 15 |
| M5-3 (1400 °C/2 h)[a] | 90.5 | 10.7 (2.0) | – | 1.8 (0.6) | – | – |
| M5-3 (1450 °C/2 h) | 91 | 13.6 (7.1) | 10 | 1.68 (0.61) | 3.5 | 11 |
| M5-3 (1500 °C/2 h) | 92 | 21 (13) | 14 | 1.69 (0.70) | 9 | 10 |
| M5-3 (1550 °C/2 h) | 92 | 24 (13) | 18 | 1.67 (0.67) | 4 | 10 |
| M5-3 (1600 °C/2 h) | 92 | 42 (18) | 37 | 1.69 (0.63) | <1 | 9 |
| M5-4 (1500 °C/2 h) | 92 | 20.0 (9.9) | 18 | 1.87 (0.81) | 1.5 | 14 |

[a] Sample difficult to polish, $S_A$ and $F_A$ measured on a small number of grains.

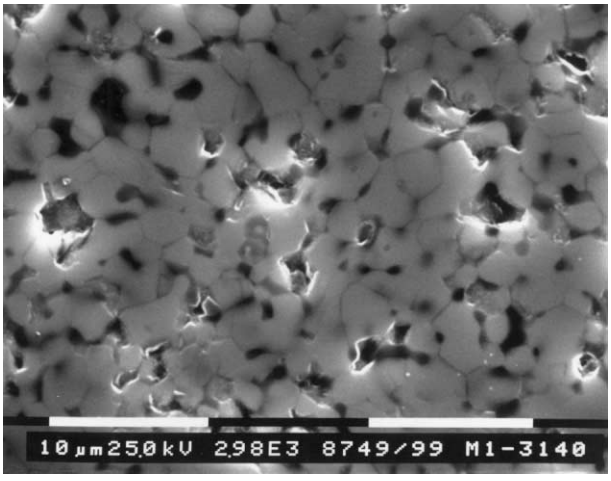


Fig. 2. Microstructure of M1-3 sintered 2 h at 1400 °C.

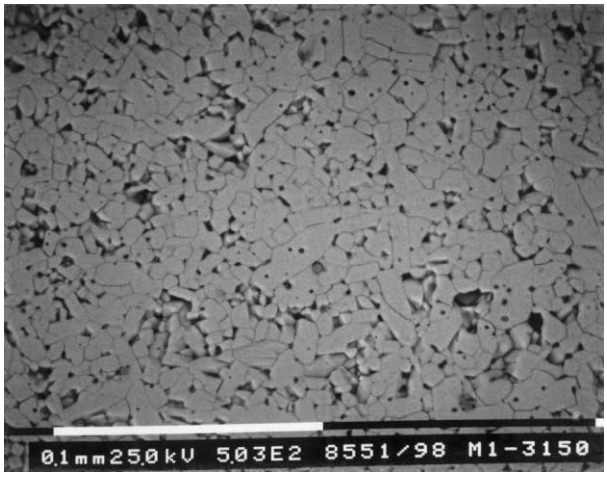


Fig. 3. Microstructure of M1-3 sintered 2 h at 1500 °C.

grains (≈10%) with shape factor >2.5. In most cases, anisotropic grain growth is also associated with exaggerated grain growth (EGG), as evident from Figs. 3, 4 and 6. However, the GSFD is never distinctly bimodal, rather a long tail is observed. As a consequence, we have arbitrarily defined the onset of EGG as the appearance of elongated grains ($F>2.5$) with size $>3S_{MF}$. This criterion matches rather well with the qualitative impression resulting from visual inspection. An extreme case is shown in Fig. 7 (M5-2, 1350 °C), where an elongated grain of ≈330 μm with shape factor ≈12 has grown in a matrix of grains <30 μm. The growth of the abnormal grains is accompanied by the trapping of large spherical pores (see Figs. 3, 4 and 6). These intragranular pores determine the rather low density of samples M5-3 and M5-4 even at high temperature (Fig. 1). The EGG process takes place generally at temperatures >1450 °C when $x=0.1$ and at temperatures ⩾1350 °C when $x=0.5$ (see Figs. 3, 4, 6 and 7). However, there are two exceptions: no EGG is observed for the M1-1 series even at 1600 °C, whereas abnormal growth begins only above 1500 °C for series

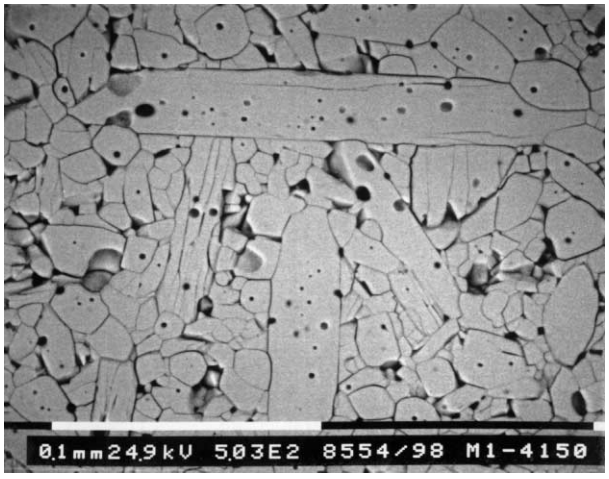


Fig. 4. Microstructure of M1-4 sintered 2 h at 1500 °C.

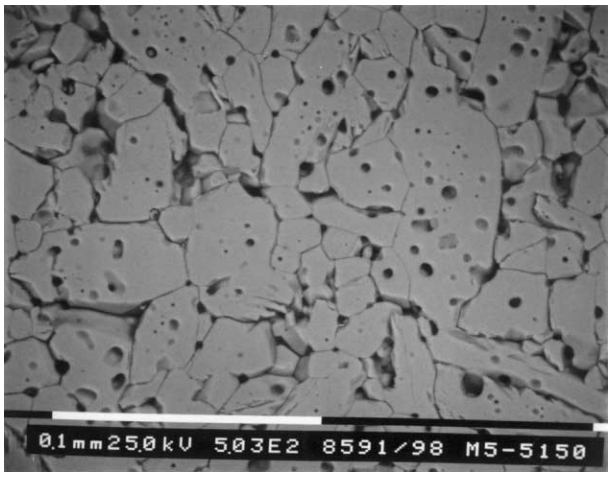


Fig. 6. Microstructure of M5-3 sintered 2 h at 1500 °C.

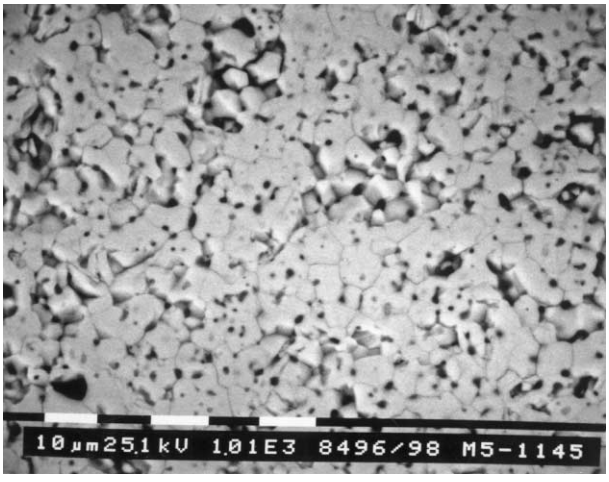


Fig. 5. Microstructure of M5-1 sintered 2 h at 1450 °C.

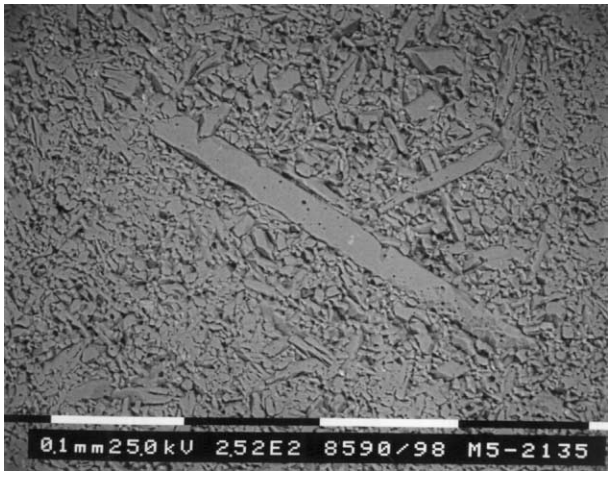


Fig. 7. Microstructure of M5-2 sintered 2 h at 1350 °C.

M5-1. Ceramics with nearly equiaxed grains ($F = 1.3$–1.4) do not show EGG (compare, for example, specimens M1-3 sintered at 1400 °C and M5-1 sintered at 1450 °C with specimens M1-3 sintered at 1500 °C and M5-3 sintered at 1500 °C in Figs. 2, 5, 3 and 6). In agreement, the percentage of grains with $S > 3S_{MF}$ and the percentage of grains with $F > 2.5$ is nil or very small in these samples. The different impact of EGG on microstructure is well evident from the GSFD. Three different situations are depicted in Fig. 8, where the frequency distribution of M5-1, M1-3 and M1-2 samples sintered at 1500 °C are compared. For sample M5-1 abnormal growth can be considered absent, although there is a small fraction (4%) of grains with size between $2S_{MF}$ and $2.5S_{MF}$. For sample M1-3 abnormal growth is restricted to a few grains with size up to $\approx 5S_{MF}$. On the contrary, for sample M1-2, EGG is much more pronounced and some grains become one order of magnitude larger than the mode of the distribution. Very broad GSFDs are also observed for series M1-3 sintered at 1550 °C and for series M1-4 and M5-3 sintered at 1500 °C. The dispersion of the grain size results in abnormally high values of the corresponding standard deviation (see Table 3). Ceramics containing 1 mol% MgO have nearly equiaxed grains and do not show EGG even at 1600 °C.

The different extent of microcracking as a function of grain size is evident from visual inspection of microstructure. When the grain size is of the order of 2–3 μm, only isolated microcracks or systems of two/three microcracks meeting at triple junctions are generally observed at grain boundaries (see Fig. 2). When the grain size increases to 4–6 μm the microcracks comprise up to 5–6 grain boundaries (see Fig. 5). For even larger grain sizes, the samples are severely microcracked with formation of complex networks of interconnected fractures (see Figs. 3, 4 and 6) which affect a large fraction of the grain boundaries. Transgranular cracks are observed on some samples (see Figs. 4 and 6), but it is not clear whether they are a result of cooling or originate during cutting and polishing.

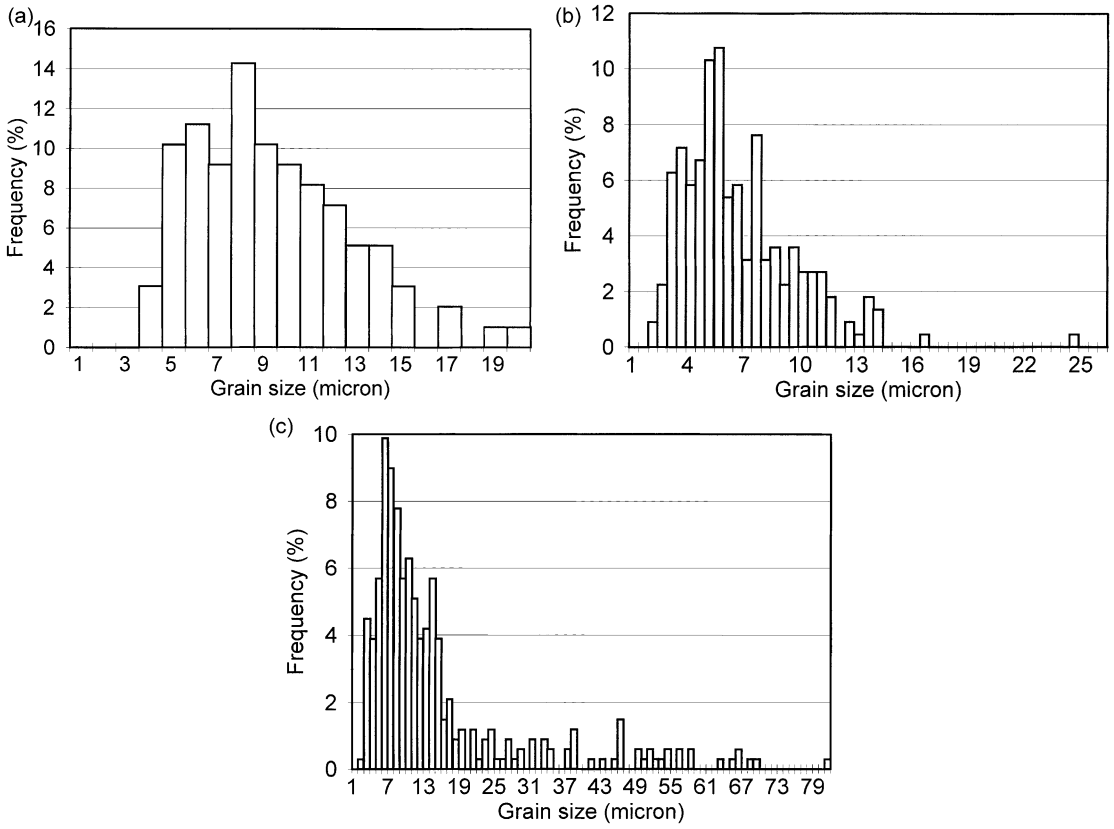


Fig. 8. Grain size frequency distribution of samples sintered at 1500 °C for 2 h. (a) M5-1, (b) M1-3, (c) M1-2.

### 3.2. Thermal expansion

Thermal expansion was measured on the samples where a quantitative microstructural characterization was conducted. Ceramics sintered at 1350 °C were excluded because of the presence of secondary phase particles. The average apparent TEC corresponding to four different temperature ranges (200–700, 800–1000, 200–1000 °C on heating and 1000–800 °C on cooling) is reported in Table 4. A quantification of thermal hysteresis was carried out by measuring the area included between the heating (elongation) and cooling (contraction) curves and dividing by the sample length. Below 150 °C the measured expansion was affected by an instrumental artefact and the initial portion of the hysteresis curve was excluded from integration. Since the thermal expansion anisotropy of $MgTi_2O_5$ is lower than that of $Al_2TiO_5$, a significant decrease of the hysteresis is expected for the solid solution $x=0.5$. However, inspection of Table 4 shows that the thermal expansion behaviour is complex and cannot be simply interpreted on the basis of the thermal expansion anisotropy. For sake of simplicity, it is convenient to separately analyze the behaviour of the two solid solutions.

#### 3.2.1. $Al_{1.8}Mg_{0.1}Ti_{1.1}O_5$

When the grain size is lower than ≈10 μm, the observed behaviour closely corresponds to the thermal expansion expected for pure $Al_2TiO_5$ or $Al_2TiO_5$ containing a limited amount of additives. An example is shown in Fig. 9 (M1-1, 1500 °C). The expansion coefficient between 200 and 1000 °C is roughly constant and close to zero, although, for other samples, it can be either slightly negative or slightly positive (see Table 4). This means that the expansion of the individual grains is largely accommodated by the existing microcracks which progressively close upon heating. The absence of a significant length variation even at high temperature can be interpreted as an expansion along the *b* and *c* directions almost exactly compensated by contraction along the *a* direction. During the cooling from 1000 to 800 °C, the samples considerably contract with a TEC of the order of $4–5\times10^{-6}$ $K^{-1}$. This value is lower than the average expansion coefficient $\overline{\alpha}$ of $Al_2TiO_5$: $9.2\times10^{-6}$ $K^{-1}$.[1] Thus, even at 1000 °C, some microcracks are not yet completely closed. Below ≈500 °C the samples begin to expand and this corresponds to the introduction of new microcracks and/or to the propagation of existing ones. The resulting hysteresis is generally very high, 0.6–1.2 K (see Table 4).

Table 4
Grain size, thermal expansion ($\alpha$) and thermal hysteresis of sintered samples

| Sample | Average grain size (μm) | $10^6\ \alpha\ (K^{-1})$ 200–700 °C | $10^6\ \alpha\ (K^{-1})$ 800–1000 °C | $10^6\ \alpha\ (K^{-1})$ 200–1000 °C | $10^6\ \alpha\ (K^{-1})$ 1000–800 °C | Hysteresis per unit length (K) |
|---|---|---|---|---|---|---|
| $Al_{1.8}Mg_{0.1}Ti_{1.1}O_5$ | | | | | | |
| M1-1 (1500 °C/2 h) | 3.3 | 0.004 | 0.003 | 0.004 | 4.36 | 0.625 |
| M1-2 (1500 °C/2 h) | 14 | −0.55 | 0.45 | −0.26 | 3.31 | 0.341 |
| M1-3 (1400 °C/2 h) | 2.3 | −0.83 | −0.13 | −0.61 | 4.42 | 0.889 |
| M1-3 (1450 °C/2 h) | 3.8 | −0.74 | −1.02 | −0.81 | 5.12 | 1.271 |
| M1-3 (1500 °C/2 h) | 6.3 | 0.104 | 0.79 | 0.29 | 5.79 | 1.136 |
| M1-3 (1550 °C/2 h) | 15 | 1.02 | 2.86 | 1.54 | 7.28 | 0.638 |
| M1-3 (1600 °C/2 h) | 19.5 | 0.76 | 1.89 | 0.95 | 4.61 | 0.312 |
| M1-3 (1600 °C/24 h) | 79.2 | 1.71 | 2.77 | 2.11 | 5.00 | 0.237 |
| M1-3 (1600 °C/100 h) | 111 | 5.42 | 5.66 | 5.51 | 6.21 | 0.324 |
| M1-4 (1500 °C/2 h) | 9.3 | −0.11 | 3.88 | 1.03 | 5.76 | 0.336 |
| $AlMg_{0.5}Ti_{1.5}O_5$ | | | | | | |
| M5-1 (1450 °C/2 h) | 4.4 | 2.69 | 4.08 | 3.22 | 7.66 | 0.585 |
| M5-1 (1500 °C/2 h) | 8.8 | 2.28 | 3.57 | 2.83 | 7.17 | 0.378 |
| M5-2 (1500 °C/2 h) | 31 | 0.90 | 1.73 | 1.22 | 3.60 | 0.169 |
| M5-3 (1400 °C/2 h) | 10.7 | 1.56 | 3.89 | 2.43 | 7.31 | 0.397 |
| M5-3 (1450 °C/2 h) | 13.6 | 2.21 | 4.47 | 2.94 | 7.71 | 0.359 |
| M5-3 (1500 °C/2 h) | 21 | 3.23 | 7.53 | 4.45 | 8.52 | 0.209 |
| M5-3 (1550 °C/2 h) | 24 | 4.94 | 8.37 | 6.14 | 9.92 | 0.316 |
| M5-3 (1600 °C/2 h) | 42 | 2.62 | 7.18 | 3.86 | 8.82 | 0.222 |
| M5-4 (1500 °C/2 h) | 20.0 | 1.12 | 3.18 | 1.78 | 5.26 | 0.188 |

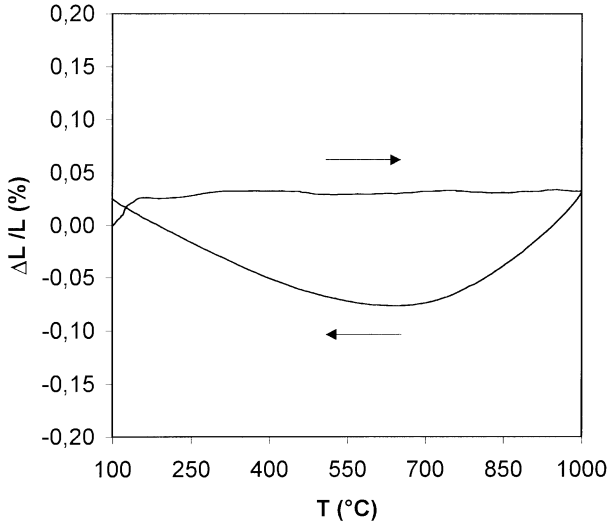


Fig. 9. Thermal expansion (contraction) of M1-1 sintered at 1500 °C for 2 h. Heating and cooling rate: 3 °C $min^{-1}$.

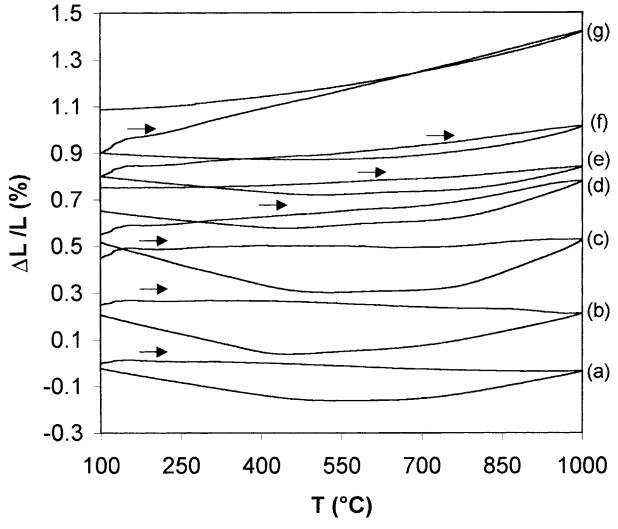


Fig. 10. Thermal expansion (contraction) of M1-3 sintered in different conditions. (a) 1400 °C, 2 h; (b) 1450 °C, 2 h; (c) 1500 °C, 2 h; (d) 1550 °C, 2 h; (e) 1600 °C, 2 h; (f) 1600 °C, 24 h; (g) 1600 °C, 100 h. Heating and cooling rate: 3 °C $min^{-1}$. The different hysteresis curves were opportunely shifted along the vertical axis for better observation.

When the grain size exceeds ≈10 μm, the thermal hysteresis decreases to ≈0.3 K and the TEC in the range 800–1000 °C increases above $2\times10^{-6}\ K^{-1}$ and is higher than in the range 200–700 °C (see Table 4). The influence of sintering conditions on thermal expansion hysteresis is shown in Fig. 10, where the behaviour of samples M1-3 sintered between 1400 and 1600 °C is compared. A strong decrease of the thermal hysteresis can be observed when the sintering temperature changes from 1500 to 1550 °C. If the TEC is plotted against the logarithm of the grain size, as shown in Fig. 11, a significant correlation is found. The increase of the apparent TEC with grain size is in particular evident for grain sizes above 10 μm. This result contradicts the behaviour generally reported in the literature about the decrease of thermal expansion with grain size. However, it should be noted that sintered ceramics with grain size exceeding

10 μm were rarely investigated. Inspection of Table 3 shows that the shape factor generally increases with grain size; the coarse grained specimens are those sintered at higher temperature where anisotropic grain growth is more pronounced. The increase of TEC in coarse grained ceramics is thus to be mainly related to the increase of $F_A$. Sample M1-2, which has the lowest $F_A$ value (1.6) among coarse grained samples, presents a TEC ($-0.26\times10^{-6}$ $K^{-1}$) comparable with that of fine grained materials. However, the experimental data in Fig. 11 are spread over a broad band rather than concentrated on a straight line and this reflects the influence of other microstructural features, like the width of the GSFD, the existence of abnormal grains and, in general, the sensitivity of microstructure evolution on the precursor powders. An additional feature of the coarse grained ceramics is the elongation of the sample after the thermal cycle in comparison to the original size. This is especially evident for the sample M1-3 sintered at 1600 °C for 100 h (see curve "g" in Fig. 10). The sample expands on heating with a constant TEC of $5.5\times10^{-6}$ $K^{-1}$, and shows a very small hysteresis down to 600 °C. At lower temperature, contraction occurs with a TEC of $\approx2\times10^{-6}$. As a consequence, the sample at room temperature after cooling is ≈0.2% longer than before heating. The same behaviour was observed on coarse-grained samples of the Mg-rich solid solution.

### 3.2.2. $AlMg_{0.5}Ti_{1.5}O_5$

In this case, the behaviour of samples with grain size up to ≈14 μm closely corresponds to that of magnesium dititanate.[4] The expansion curve (an example is shown in Fig. 12) has four distinct features. Between 200 and 700 °C the samples moderately expand with $\alpha\approx2\times10^{-6}$ $K^{-1}$. As the temperature further increases, the expansion is more pronounced and $\alpha\approx3$–$4\times10^{-6}$ $K^{-1}$. The increase of TEC probably indicates that a consistent fraction of the microcracks along *a* and *b* directions are probably healed at this point. On cooling, the samples initially contract with $\alpha\approx7\times10^{-6}$ $K^{-1}$. This figure is close to the value of $\overline{\alpha}$ for $MgTi_2O_5$ : $7.9\times10^{-6}$ $K^{-1}$.[1] Under the assumption of a linear dependence of the thermal expansion along the principal crystallographic directions on composition, the value of $\overline{\alpha}$ expected for $AlMg_{0.5}Ti_{1.5}O_5$ is $8.5\times10^{-6}$ $K^{-1}$. As a consequence, most of the microcracks are healed at 1000 °C. Below ≈400 °C, microcracks are re-introduced in the sample and a small expansion is observed. The overall behaviour of samples is dominated by the smaller anisotropy of TEC in comparison to pure $Al_2TiO_5$. This in turn

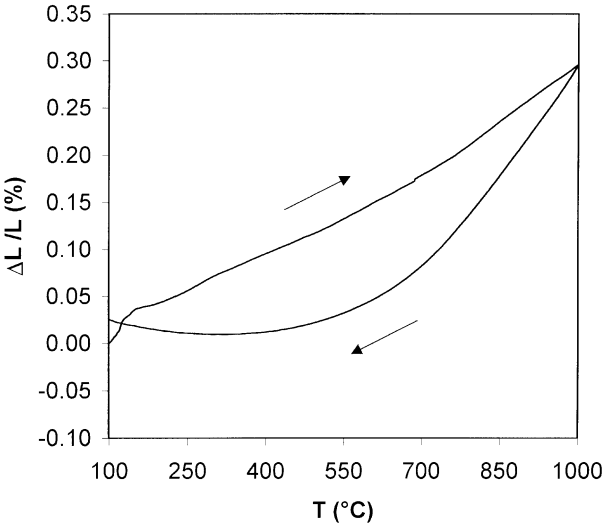


Fig. 12. Thermal expansion (contraction) of M5-1 sintered at 1450 °C for 2 h. Heating and cooling rate: 3 °C $min^{-1}$.

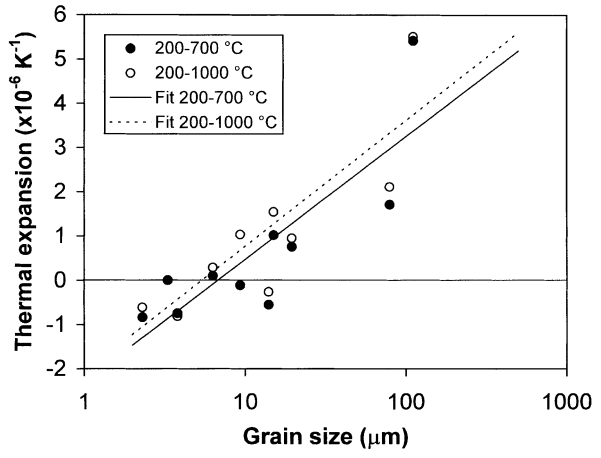


Fig. 11. Apparent thermal expansion coefficient of ceramics $Mg_{0.1}Al_{1.8}Ti_{1.1}O_5$. (●) Average TEC between 200 and 700 °C. (○) Average TEC between 200 and 1000 °C. Solid line: best fit to 200–700 °C data. Dotted line: best fit to 200–1000 °C data.

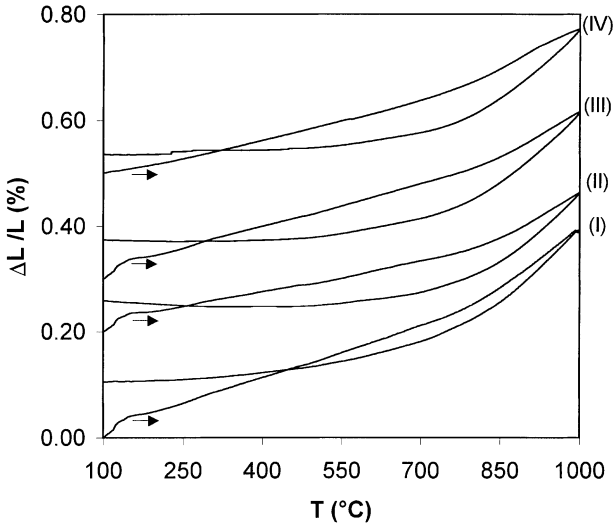


Fig. 13. Effect of thermal cycling (roman numerals) on hysteresis of M5-3 sintered at 1500 °C for 2 h. The different hysteresis curves were opportunely shifted along the vertical axis for better observation.

reflects on a larger expansion on heating and a reduced thermal hysteresis (0.4–0.6 K). Samples with grain size $>20$ μm are characterized by a lower hysteresis (0.17–0.32 K) and show a more complex behaviour. For samples of the M5-3 series, the TEC in the range 800–1000 °C increases to $7–8\times10^{-6}$ $K^{-1}$. As in the case of samples M1-3 sintered above 1500 °C, the room temperature size after cooling is significantly larger (0.15%) than before heating. In contrast to materials of composition $Al_{1.8}Mg_{0.1}Ti_{1.1}O_5$, a significant correlation between the grain size and the apparent TEC is not observed.

An additional feature of large-grained samples of both compositions is their sensitivity to thermal cycling. A significant variation of the hysteresis curve is observed if successive heating and cooling cycles are performed, as shown in Fig. 13 for what concerns sample M5-3 sintered at 1500 °C (grain size: 21 μm). Hysteresis increases of about 40% during the second thermal cycle (0.295 K) in comparison to the first one (0.209 K), while progressively smaller variations are observed on the third (0.327 K) and fourth (0.309 K) cycle. For each cycle, an increase of the sample length after cooling is observed. For samples with smaller grain size ($<10$ μm), there is not appreciable length increase after cooling and the thermal behaviour obtained in two successive cycles is roughly comparable; the variation of the hysteresis is typically $\leqslant10\%$.

## 4. Discussion

Magnesium oxide plays a critical role in microstructure evolution of reaction sintered aluminium titanate.[24–26] Reaction sintering of pure $Al_2TiO_5$ from $Al_2O_3$ and $TiO_2$ often produces porous and coarse-grained ceramics. The different microstructure evolution is related to distinct solid-state mechanisms. In the case of pure $Al_2TiO_5$, owing to the low driving force available for the formation of the pseudobrookite phase, growth of $Al_2TiO_5$ occurs only at a limited number of centres of easier nucleation, with formation of a coarse microstructure.[27] In this case, microstructure is mainly determined during the reaction stage. The addition of MgO provides a large number of nucleation centres for the formation of the pseudobrookite phase; as a consequence microstructure evolution is controlled by sintering and grain growth rather than by reaction.[24–27] However, reaction sintering must be carried out at a temperature lower than that corresponding to the onset of exaggerated grain growth to have an effective control on microstructure evolution, but high enough to avoid the presence of unreacted particles. For the solid solution with $x=0.1$, this is possible by sintering in the temperature range 1400–1500 °C. The resulting ceramic bodies have rather high density ($\geqslant90\%$), reduced grain size (2–6 μm), low thermal expansion ($-0.8$ to $0.3\times10^{-6}$ $K^{-1}$, 200–1000 °C) and rather reproducible expansion behaviour. For the Mg-rich solid solution ($x=0.5$) microstructure is more difficult to control owing to premature onset of EGG. For most of the samples (except M5-1 series) abnormal grain growth already occurs at 1350 °C. If sintering were carried out at lower temperatures it would result in a large amount of secondary phases ($MgAl_2O_4$ and $TiO_2$). In addition, owing to the reduced thermal expansion anisotropy in comparison to $Mg_{0.1}Al_{1.8}Ti_{1.1}O_5$, the TEC (200–1000 °C) is increased to $2–3\times10^{-6}$ $K^{-1}$.

EGG is observed in connection to anisotropic grain growth and is probably related to the localized formation of small quantities of liquid or glassy phase owing to the presence of silica impurities in the starting raw materials. The main source of silica are the $TiO_2$ powders; both have a $SiO_2$ content of the order of 1000 ppm (ICP analysis). The formation of liquid or glassy phase in the $MgO–SiO_2–Al_2O_3$ system begins to occur at temperatures slightly above 1350 °C.[28] The existence of a glassy phase at grain boundaries and triple points has been well documented by Wohlfromm et al.[29] in their TEM study on microstructure of reaction sintered aluminum titanate. The microstructure reported for a sample containing ≈10 mol% of $MgTi_2O_5$ sintered at 1450 °C clearly shows large elongated grains (up to ≈80 μm) typical of EGG. Excess silica was also found to promote anisotropic grain growth of $Al_2TiO_5$ during sintering of composite materials containing 25 vol.% mullite.[30] In the present case, the tendency to abnormal grain growth increases with the amount of MgO; ceramics prepared with the addition of only 1 mol% MgO ($x=0.01$) do not show EGG even at 1600 °C and the final microstructure is quite insensitive to the nature of the precursor powders. On the contrary, for solid solutions with $x=0.1$ and $x=0.5$, the impact of EGG on microstructure evolution is strongly dependent on the nature of the oxide precursors; in general, samples prepared from the M1 kind of magnesium oxide are less sensitive to EGG. This is an indication that other impurities in addition to $SiO_2$ and MgO contribute to the formation of the liquid/glassy phase. EGG can be suppressed or, al least, controlled by addition of a second phase. Composite materials, containing alumina or mullite,[25,30–32] have a finer and more uniform microstructure than single phase aluminium titanate ceramics. The second phase leads to an improvement of the mechanical strength, but also to an increase of the thermal expansion coefficient and a reduction of thermal shock resistance.[31,32]

From the point of view of thermal expansion, ceramics with grain size of 2–6 μm should represent a good compromize between low thermal expansion and the extent of microcracking. According to the empirical relationship derived by Ohya et al.,[33]

$$V_{cr} = 10^{0.16} G^{0.5} \quad (1)$$

the percentage crack volume at room temperature, $V_{cr}$, is proportional to the square root of grain size, $G$. Eq. (1) yields $V_{cr} = 2.0\%$ for $G = 2$ μm; $V_{cr} = 2.8\%$ for $G = 4$ μm and $V_{cr} = 4.6\%$ for $G = 10$ μm. Microstructure observation qualitatively supports the trend described by the above relationship; the microcrack density gradually increases with grain size. However, when the grain size exceeds ≈10 μm the samples are extensively microcracked and further variation of microcrack density is hardly appreciable. In the case of composition $Mg_{0.1}Al_{1.8}Ti_{1.1}O_5$ the TEC on heating (200–1000 °C) is in the range −0.8 to $0.3\times10^{-6}$ $K^{-1}$ for a grain size of 2–6 μm while it increases above $1\times10^{-6}$ $K^{-1}$ for coarser microstructures (see Fig. 11). The temperature (in °C) at which microcracking begins, $T_{mc}$, can be obtained from the energy criterion originally proposed by Cleveland and Bradt[13] and later developed by other Authors.[15,16,33] In particular, Ohya et al.[15,33] have obtained

$$T_{mc} = K' G^{-0.5} + T_0 \quad (2)$$

where $K' \approx -1800$ °C $\mu m^{0.5}$. The temperature at which elastic stresses are no longer relieved by plastic deformation in aluminium titanate is of the order of 1500 °C;[15,33] as a consequence, following the suggestion of Ohya and coworkers, for samples sintered at temperature ⩽1500 °C, the term $T_0$ can be equated to the sintering temperature. If $T_0 = 1500$ °C, microcracking will occur below room temperature if the grain size is smaller than ≈1.5 μm.

The observed strong decrease of thermal hysteresis above a certain grain size (see Fig. 10 and Table 4) corresponds to the transition from a microstructure where none or only a few microcracks are still open at 1000 °C to an extensively microcracked microstructure (at the same temperature). The critical grain size can be estimated by putting $T_{mc} = 1000$ °C and $T_0 = 1500$ °C in Eq. (2) and results ≈13 μm. This is in satisfactory agreement with the experimental results; in the case of samples M1-3, the decrease of hysteresis (see Fig. 10) is observed when moving from a grain size of 6.3 μm (sintering temperature 1500 °C) to a grain size of 15 μm (sintering temperature 1550 °C). The values of $K'$ and $T_0$ were derived[15,33] for pure $Al_2TiO_5$ or materials containing only a small amount of additives; probably different values applies to $AlMg_{0.5}Ti_{1.5}O_5$. An increase of the critical size corresponding to the transition from a crack free to a extensively microcracked microstructure at 1000 °C with the amount of $MgTi_2O_5$ is expected; in agreement, in the case of M5-3 samples, the reduction in hysteresis was observed between 14 and 21 μm.

While the thermal expansion of fine-grained samples can be assimilated to that expected for the prototype ceramics $Al_2TiO_5$ and $MgTi_2O_5$, the behaviour of coarse-grained ceramics is more complex and less systematic. In particular, there is some evidence that the apparent TEC is affected by the shape factor of the grains for the composition $Mg_{0.1}Al_{1.8}Ti_{1.1}O_5$. High sintering temperatures and longer times promote anisotropic grain growth and the development of coarse microstructures. The observed increase of the TEC, in particular above the grain size of 10 μm, indicated a change of the microcracking behaviour. Large elongated grains in microcracked bodies appear to be mainly connected along one of the crystallographic directions (*b* or *c*) with positive expansion coefficient. In contrast, relatively small equiaxed grains should be connected mainly along the *a* direction, because the apparent TEC is slightly negative or close to zero. The existence of isolated grains much larger than the average grain size in some samples, as a result of EGG, is expected to affect the thermal expansion . These abnormally large grains can create a system of localized stresses within the sintered body during cooling. Thus, the increase in length of the large grained samples after cooling from 1000 °C could be interpreted as the development of macroscopic cracks related to very large grains. In agreement, coarse grained samples are quite weak, even though they do not break spontaneously. Some similarities exist with the study of Dole et al.[11] on the microcracking of monoclinic $HfO_2$, where a complex expansion (contraction) behaviour (unstable microcracks) was reported for specimens with an extremely high degree of microcracking. The presence of a complex network of interconnected microfractures rather than of isolated microcracks owing to the large fraction of microcracked grain boundaries, and the interaction between intersecting cracks can also affect the overall behaviour of coarse-grained ceramics. However, a detailed analysis of the effects of the aforementioned factors is beyond the purpose of this work.

## 5. Summary

Polycrystalline bodies of composition $Mg_{0.1}Al_{1.8}Ti_{1.1}O_5$ and $Mg_{0.5}AlTi_{1.5}O_5$ were prepared by reaction sintering at temperatures of 1350–1600 °C starting from mixtures of the parent binary oxides. During cooling from the sintering temperature, microcracking develops and the final materials show a low thermal expansion. Microstructure was characterized by measuring the grain size frequency distribution and the shape factor frequency distribution. Thermal expansion hysteresis between 200 and 1000 °C was studied by means of dilatometry. The experimental results lead to the following conclusions.

Ceramics of composition $Mg_{0.1}Al_{1.8}Ti_{1.1}O_5$ with high relative density (⩾90%), reduced grain size (2–6 μm), low thermal expansion (−0.8 to $0.3\times10^{-6}$ $K^{-1}$) and

rather reproducible expansion behaviour can be obtained by reaction sintering at 1400–1500 °C. At higher temperature, microstructure evolution is dominated by anisotropic and exaggerated grain growth with a rapid increase of the grain size.

Ceramics with composition $Mg_{0.5}AlTi_{1.5}O_5$ are characterized by the premature onset of exaggerated grain growth, which is already active at 1350 °C. Therefore, materials with grain size $< 5$ μm are difficult to obtain with conventional reaction sintering. The average thermal expansion coefficient between 200 and 1000 °C for the finest grained samples is of the order of $2–3\times10^{-6}$ $K^{-1}$.

The onset of exaggerated grain growth corresponds to the appearance of elongated grains with shape factor $>2.5$ and size $>3S_{MF}$, where $S_{MF}$ is the mode of the grain size distribution. The fraction of abnormal grains at a given sintering temperature and the corresponding growth rate strongly depend on the nature of the starting oxides.

For both compositions, a significant decrease of hysteresis was observed when the grain size exceeds 10–15 μm. Above this critical size, microcracks healing only occurs above 1000 °C. Coarse grained materials show a significant variation of the thermal expansion hysteresis with thermal cycling. In addition, a length increase of the samples in comparison to the initial size was observed after heating to 1000 °C and cooling down. Coarse grained ceramics of composition $Mg_{0.1}Al_{1.8}Ti_{1.1}O_5$ also exhibit an increase of the apparent TEC ($>1\times10^{-6}$ $K^{-1}$) in comparison to fine grained samples related to anisotropic grain growth.

## Acknowledgements

The authors wish to thank Professor Pedro Mantas (University of Aveiro, Portugal) for fruitful discussions and suggestions. This research was supported, in part, by the Italian Space Agency.

## References

1. Bayer, G., Thermal expansion characteristics and stability of pseudobrookite-type compounds, $Me_3O_5$. *J. Less-Common Met.*, 1971, **24**, 129–138.
2. Morosin, B. and Lynch, R. W., Structure studies on $Al_2TiO_5$ at room temperature and at 600 °C. *Acta Crystallogr.*, 1972, **B28**, 1040–1046.
3. Buessem, W. R., Thielke, N. R. and Sarakauskas, R. V., Thermal expansion hysteresis of aluminum titanate. *Ceram. Age*, 1952, **60**, 38–40.
4. Kuszyc, J. A. and Bradt, R. C., Influence of grain size on effects of thermal expansion anisotropy in $MgTi_2O_5$. *J. Am. Ceram. Soc.*, 1973, **56**, 420–423.
5. Ohya, Y., Nakagawa, Z. and Hamano, K., Crack healing and bending strength of aluminum titanate ceramics at high temperature. *J. Am. Ceram. Soc.*, 1988, **71**, C232–C233.
6. Siebeneck, H. J., Hasselman, D. P. H., Cleveland, J. J. and Bradt, R. C., Effect of microcracking on the thermal diffusivity of $Fe_2TiO_5$. *J. Am. Ceram. Soc.*, 1976, **59**, 241–244.
7. Hasselman, D. P. H., Donaldson, K. Y., Anderson, E. M. and Johnson, T. A., Effect of thermal history on the thermal diffusivity and thermal expansion of an alumina-aluminum titanate composite. *J. Am. Ceram. Soc.*, 1993, **76**, 2180–2184.
8. (a) Bush, E. A. and Hummel, F. A., High temperature mechanical properties of ceramic materials: I. *J. Am. Ceram. Soc.*, 1958, **41**, 189–195; (b) Bush, E. A. and Hummel, F. A., High temperature mechanical properties of ceramic materials: II. *J. Am. Ceram. Soc.*, 1959, **42**, 388–391.
9. Manning, W. R. and Hunter Jr., O., Anomalous elastic behaviour of polycrystalline $Nb_2O_5$. *J. Am. Ceram. Soc.*, 1973, **56**, 602–603.
10. Malarkey, C. J. and Hunter Jr., O., Microcracking of $Eu_2O_3$-$Ta_2O_5$ bodies. *J. Am. Ceram. Soc.*, 1978, **61**, 315–317.
11. Dole, S. L., Hunter Jr., O., Calderwood, F. W. and Bray, D. J., Microcracking of monoclinic $HfO_2$. *J. Am. Ceram. Soc.*, 1978, **61**, 486–490.
12. Holcombe, C. E. Jr. and Smith, D. D., Characterization of the thermally contracting tungstates $Ta_{22}W_4O_{67}$, $Ta_2WO_8$ and $Ta_{16}W_{18}O_{94}$. *J. Am. Ceram. Soc.*, 1978, **61**, 163–169.
13. Cleveland, J. J. and Bradt, R. C., Grain size/microcracking relations for pseudobrookite oxides. *J. Am. Ceram. Soc.*, 1978, **61**, 478–481.
14. Parker, F. J. and Rice, R. W., Correlation between grain size and thermal expansion for aluminum titanate materials. *J. Am. Ceram. Soc.*, 1989, **72**, 2364–2366.
15. Ohya, Y., Nakagawa, Z. and Hamano, K., Grain-boundary microcracking due to thermal expansion anisotropy in aluminum titanate ceramics. *J. Am. Ceram. Soc.*, 1987, **70**, C184–C186.
16. Case, E. D., Smyth, J. R. and Hunter, O., Grain-size dependence of microcrack initiation in brittle materials. *J. Mater. Sci.*, 1980, **15**, 149–153.
17. Krstic, V. D. and Vlajic, M. D., Conditions for spontaneous cracking of a brittle matrix due to the presence of thermoelastic stresses. *Acta Metall.*, 1983, **31**, 139–144.
18. Krstic, V. D., Fracture of brittle solids in the presence of thermoelastic stresses. *J. Am. Ceram. Soc.*, 1984, **67**, 589–593.
19. Meléndez-Martínez, J. J., Jeménez-Melendo, M., Domínquez-Rodríquez, A. and Wötting, G., High temperature mechanical behaviour of aluminium titanate—mullite composites. 2001, **21**, 63–70.
20. Thomas, H. A. J. and Stevens, R., Aluminium titanate—a literature review part 2: engineering properties and thermal stability. *Br. Ceram. Trans.*, 1989, **88**, 184–190.
21. Ishitsuka, M., Sato, T., Endo, T. and Shimada, M., Synthesis and thermal stability of aluminum titanate solid solutions. *J. Am. Ceram. Soc.*, 1987, **70**, 69–71.
22. Buscaglia, V., Battilana, G., Leoni, M. and Nanni, P., Decomposition of $Al_2TiO_5$-$MgTi_2O_5$ solid solutions: a thermodynamic approach. *J. Mater. Sci.*, 1996, **31**, 5009–5016.
23. Buscaglia, V. and Nanni, P., Decomposition of $Al_2TiO_5$ and $Al_{2(1-x)}Mg_xTi_{(1+x)}O_5$ ceramics. *J. Am. Ceram. Soc.*, 1998, **81**, 2645–2653.
24. (a) Buscaglia, V., Nanni, P., Battilana, G., Aliprandi, G. and Carry, C., Reaction sintering of aluminium titanate: I—effect of MgO addition, *J. Eur. Ceram. Soc.*, 1994, **13**, 411–417; (b) Buscaglia, V., Nanni, P., Battilana, G., Aliprandi, G. and Carry, C., Reaction sintering of aluminium titanate: II—effect of different alumina powders, *J. Eur. Ceram. Soc.*, 1994, **13**, 419–426.
25. Buscaglia, V., Alvazzi DelFrate, M., Nanni, P., Leoni, M. and Bottino, C., Factors affecting microstructure evolution during reaction sintering of $Al_2TiO_5$ ceramics. In *Ceramics: Charting the Future, Proceedings of the 8th CIMTEC—World Ceramic Congress*, ed. P. Vincenzini. Techna, Faenza, Italy, 1994, pp. 1867–1874.
26. Buscaglia, V., Alvazzi DelFrate, M., Leoni, M., Bottino, C. and Nanni, P., The effect of $MgAl_2O_4$ on the formation kinetics of

$Al_2TiO_5$ from $Al_2O_3$ and $TiO_2$ fine powders. *J. Mater. Sci.*, 1996, **31**, 1715–1724.
27. Freudenberg, B. and Mocellin, A., Aluminum titanate formation by solid-state reaction of fine $Al_2O_3$ and $TiO_2$ powders. *J. Amer. Ceram. Soc.*, 1987, **70**, 33–38.
28. Levin, E. M., Robbins, C. R. and McMurdie, H. F., *Phase Diagrams for Ceramists*. The American Ceramic Society, Columbus, OH, 1964 (p. 246)..
29. Wohlfromm, H., Epicier, T., Moya, J. S., Pena, P. and Thomas, G., Microstructural characterization of aluminum titanate-based composite materials. *J. Eur. Ceram. Soc.*, 1991, **7**, 385–396.
30. Huang, Y. X., Senos, A. M. R. and Baptista, J. L., Effect of excess $SiO_2$ on the reaction sintering of aluminium titanate-25 vol% mullite composites. *Ceram. Int.*, 1998, **24**, 223–228.
31. Lee, H. L., Jeong, J. Y. and Lee, H. M., Preparation of $Al_2TiO_5$ from alkoxides and the effect of additives on its properties. *J. Mater. Sci.*, 1997, **32**, 5687–5695.
32. Huang, Y. X., Senos, A. M. R. and Baptista, J. L., Thermal and mechanical properties of aluminium titanate-mullite composites. *J. Mater. Res.*, 2000, **15**, 357–363.
33. Ohya, Y. and Nakagawa, Z., Measurement of crack volume due to thermal expansion anisotropy in aluminium titanate ceramics. *J. Mater. Sci.*, 1996, **31**, 1555–1559.